Phylogeny and Expression of Canonical Transient Receptor Potential (TRPC) Genes in Developing Zebrafish

Authors, affiliations and grants:

Valentin von Niederhäusern[†], Edda Kastenhuber[†], Andreas Stäuble, Matthias Gesemann, Stephan C.F. Neuhauss*

University of Zurich, Institute of Molecular Life Sciences, Neuroscience Center Zurich and Center for Integrative Human Physiology, Winterthurerstrasse 190, CH-8057 Zurich, Switzerland

[†]Valentin von Niederhäusern and Edda Kastenhuber contributed equally to this work.

*Correspondence to: Stephan C.F. Neuhauss, Institute of Molecular Life Sciences, University of Zurich, Winterthurerstrasse 190, CH-8057 Zurich, Switzerland. Ph: +41 44 6356040; Fax. +41 44 6356897; Email: stephan.neuhauss@imls.uzh.ch

Grant sponsor: EMBO ALTF 326-2010 (EK); Swiss National Science Foundation 31003A_135598/1; EU FP7 ZF-HEALTH

Running title: TRPC genes in developing zebrafish

Keywords: *Danio rerio*; TRPC ion channel; nervous system, sensory system

Key findings:

- The zebrafish *Danio rerio* genome hosts 12 *canonical trp* genes.
- All orthologs but *trpc1* and *trpc3* are duplicated in the zebrafish genome.
- Zebrafish *trpc* paralogs show a mostly non-overlapping expression pattern.
- The zebrafish *trpc* genes are expressed predominantly in the nervous system.
- Distinct and dynamic expression patterns in various sensory and motor systems can be detected during development.

ABSTRACT

Background: Canonical transient receptor potential (TRPC) channels are nonselective, calcium-permeable cation channels that are expressed in a great variety of organisms, tissues and cell types. TRPC channels are known to be involved in the transduction of polymodal sensory input. Additionally, they are implicated in a variety of developmental processes. Distinct gating mechanisms have been elucidated so far, but their exact functional role in vertebrate organisms still needs to be resolved.

Results: We now used the zebrafish *Danio rerio* to perform a comprehensive expression analysis of the *trpc* gene subfamily. Based on the sequence homology to the seven described mammalian TRPC channels, we identified 12 *trpc* genes in the zebrafish genome. All but *trpc1* and *trpc3* consist of two paralogs. We further describe the specific expression patterns of *trpc* transcripts in whole mounts during the first five days of development.

Conclusions: Consistent with their proposed role in sensory transduction zebrafish *trpcs* are predominantly expressed in neural structures such as the olfactory, visual, mechanosensitive, and motor systems. Intriguingly, zebrafish paralogs show mainly non-overlapping expression patterns, suggesting that duplicated genes have either split their functions or have adapted new ones.

INTRODUCTION

Many physiological and cellular processes, such as changes in membrane potential and increase in intracellular calcium, rely on the action of ion channels. The transient receptor potential (TRP) channel proteins are a distinct superfamily of widely expressed, non-selective cation channels that comprises six subfamilies in mammals (Ramsey et al., 2006; Venkatachalam and Montell, 2007; Nilius and Owsianik, 2011). The subgroup of canonical TRP channels (TRPCs) has the closest homology to the original *Drosophila* trp gene, which when mutated lead to a transient receptor potential in the visual signal transduction cascade of the fruit fly and gave the whole family its name (Minke, 2010). Seven mammalian TRPC genes have been described so far, all of which code for channel proteins containing a short, hydrophobic, pore-forming sequence between the last two of the six transmembrane domains. Homo- or heterotetrameric assembly of TRPC subunits allows the generation of a large variety of functional channels with different specificity and channel properties. Heteromerization with more distantly related subunits of different subfamilies has also been described, adding even more diversity (summarized by Cheng et al., 2010). TRPCs have been shown to be expressed in a broad range of different tissues, in both excitable and non-excitable cells (Kunert-Keil et al., 2006; Abramowitz and Birnbaumer, 2009). However, an extensive expression study localizing TRPC transcripts in a whole mount organism has not yet been carried out.

Gating mechanisms of TRPC channels are the best understood among the TRP superfamily. Channel properties were most often studied in exogenous expression systems leading to sometimes contradictory findings regarding their mode of activation (Putney, 2004; Lev et al., 2012). But the main trigger for TRPC channels is phospholipase C (PLC)-dependent, receptor-operated activation downstream of G-protein coupled receptors (GPCR), or receptor tyrosine kinases. The subsequent generation of diacylglycerol and inositol triphosphate has been implicated in direct and indirect channel activation mechanisms, respectively (reviewed by Soboloff et al., 2007; Albert, 2011). Another model

linking agonist-induced receptor activation to channel gating is the regulated delivery of the TRP protein to the plasma membrane (Bezzerides et al., 2004).

Recently, investigations in different organisms have shed light on functional implications of these cation channels. Many TRPC channels are involved in the integration of sensory information where they function as both external and internal sensors (reviewed in Clapham, 2003; Damann et al., 2008). Moreover, they play important roles during development by regulating aspects of apoptosis, neurite outgrowth, axon guidance and synapse formation (summarized in Vennekens et al., 2012). Hence it is not surprising that they have been linked to a number of human neurological diseases such as Parkinson's disease or cerebellar ataxia (Selvaraj et al., 2010). Due to their effect on proliferation and cell death, TRPC channels have also been linked to cancer (reviewed in Shapovalov et al., 2011). The vertebrate model organism zebrafish (*Danio rerio*) displays many features, including an established tool kit to study and manipulate gene expression and function as well as easy accessibility to neurons for electrophysiological recordings, which make it amenable for studies on TRPC channels.

A first step towards functional investigations, the thorough description of *trpc* genes and expression, is presented here. We report the identification of a total of 12 zebrafish orthologs. Moreover, whole mount in situ hybridization (WISH) analyses of the entire *trpc* gene subfamily during the first five days of development enabled the description of distinct and dynamic expression patterns in diverse neural structures of zebrafish embryos and early larvae.

RESULTS AND DISCUSSION

The TRPC family in the zebrafish *Danio rerio*

Using the seven human and murine *trpc* sequences as initial queries, we identified and annotated 12 *trpc* genes in the zebrafish genome (Fig. 1). Molecular cloning of the coding sequences confirmed that all of our annotated sequences are transcribed. Subsequent phylogenetic analysis indicated that all but *trpc1* and *trpc3* have retained duplicates after the teleost specific genome duplication (reviewed by Meyer and van de Peer, 2005). As duplicated genes are liberated from selective pressure due to initial functional redundancy, duplicates are often lost during evolution. However, the fact that many TRPC genes have retained their duplicates indicates that the gene functions of these paralogs many have diverged in so called sub- and/or neofunctionalization events (Postlethwait, 2007). In order to enable functional studies, we have now performed WISH experiments analyzing the expression patterns of *canonical trp* genes during embryonic and early larval development.

Broad expression of *trpc1*

Previous studies have described *trpc1* expression in the zebrafish head, retina, inner ear, and outflow tract of the heart (Möller et al., 2008; Petko et al., 2009). We extend these previous expression studies by analyzing larvae 5 days post fertilization (dpf) and add new data to a more precise expression analysis in the brain. We observe transcripts of *trpc1* to be distributed ubiquitously in the brain at 24 hpf with stronger expression in the telencephalon and diencephalon as well as in presumptive cranial sensory ganglia (CSG), (Fig. 2A, B). Staining in cranial sensory ganglia becomes even more pronounced around the third day post fertilization (Fig. 2D, E) before it ceases by 5 dpf.

Consistent with earlier reports, we detect retinal expression within the inner nuclear layer (INL) and ganglion cell layer (GCL). Expression is first observed at 48 hpf (Fig. 2C) and becomes prominent by day three, when the formation of retinal layers commences (Fig 2F). *trpc1* expressing cells are likely amacrine and retinal ganglion cells based on their location in the INL and GCL, respectively. In mice retinal expression of TRPC1 is strongly enriched in

photoreceptor inner segments but also present in other retinal layers (Gilliam and Wensel, 2011). Promising candidates for upstream activators of TRPC1 are metabotropic glutamate receptors linked to the PLC pathway as well as sphingosine-1-phosphate receptors (Morgans et al., 2009; Shen et al., 2009; Koike et al., 2010; Gleason, 2012).

From 3 dpf onwards, cells in the optic tectum (TeO) and both habenulae (Ha) start to express *trpc1* (Fig. 2G-K). Interestingly, expression in the habenulae is clearly asymmetric at 5 dpf, with higher expression levels in the left hemisphere (Fig. 2J, K). As the habenulae are known to be highly asymmetric structures with respect to their connectivity, development and molecular signature, differential gene expression patterns are often observed (reviewed by Roussigne et al., 2012). Moreover, various developmental processes such as cell proliferation, axonal pathfinding, synaptogenesis and cell survival depend on calcium signaling trough store-operated calcium channels, and TRPC1 has been identified as an important contributing channel to these events (reviewed by Tai et al., 2009, Vennekens et al., 2012). Yu and colleagues (Yu et al., 2010) observed severe defects in angiogenic sprouting of intersegmental vessels upon gene knockdown of *trpc1*. In summary, the broad expression of *trpc1* in the developing zebrafish brain suggests a role in neural development.

Expression of *trpc2* paralogs in the zebrafish olfactory system

The teleost fish olfactory system consists of an olfactory epithelium (OE) containing both ciliated and microvillous olfactory sensory neurons (OSNs; reviewed by Touhara and Vosshall, 2009). Using a transgenic approach, Sato and colleagues (Sato et al., 2005) have demonstrated that the two kinds of OSNs operate through distinct types of transduction machineries with microvillous OSNs relying on V2R receptor signaling upstream of TRPC2 channels. Consistent with this work, we found transcripts of *trpc2* in the OE. The used sequence (NCBI GenBank accession number AY974804) corresponds to our *trpc2a* paralog. Our analysis shows that OSNs start to express *trpc2a* from the first day of development up to at least 5 days post fertilization (Fig. 3 A-E). Expression of *trpc2b* shows a similar time

course but is confined to a different subpopulation of OSNs comprising fewer cells located in the distal part of the OE (Fig. 3F-K).

In rodents, TRPC2 has been shown to play a crucial role in pheromone detection by the microvillous sensory neurons of the vomeronasal organ (VNO), which express genes of the V1R- or V2R-families of putative pheromone receptors as well as TRPC2 (Liman et al., 1999; Dulac and Torello, 2003). Several studies have shown remarkable defects in social and sexual behavior in TRPC2 deficient mice (Leypold et al., 2002; Stowers et al., 2002; Lucas et al., 2003). In contrast, human TRPC2 is only present as a pseudogene whose inactivation likely occurred during primate evolution (Liman and Innan, 2003). Even though zebrafish do not possess a vomeronasal organ, there is evidence that they use a wide range of chemicals as pheromone signals (Sorensen and Stacey, 2004; Hashiguchi et al., 2008). The physiological segregation of olfactory pathways in zebrafish points towards a functional separation in the perception of different chemical compounds, suggesting pheromone sensing to be mediated at least partially by TRPC2 expressing microvillous OSNs. The identity of the V2R receptors acting upstream of the channel and especially activators of the signal transduction cascade remain to be determined.

trpc3 is expressed in major motor components

Our *in situ* hybridization experiments revealed a highly dynamic expression of *trpc3* during the first days of development. At 24 hpf, *trpc3* is expressed in two small, bilateral cell clusters in the dorsal telencephalon and the ventral diencephalon (Fig. 4A, B). Further staining can be found in bilaterally arranged cells in rhombomeres 5 and 6 (R5, R6) and in a population of primary motor neurons aligned in a segmented manner along the spinal cord (Fig. 4C-E). At 48 hpf, expression in spinal motor neurons persists and several additional expression domains in the hindbrain become detectable, including staining in several clusters of presumptive reticulospinal neurons and hindbrain motoneurons (Fig. 4F-J). Low levels of *trpc3* transcripts are also detected in the pretectum (Pr) and the olfactory bulb (OB, Fig. 4F, G). Expression in sparse cells within the eye, located ventrally to and in proximity of

the lens was detected transiently at 48hpf (Fig. 4K). Based on the location near the optic fissure and the temporally restricted expression, these cells might represent a subset of differentiating retinal neurons. At 3 dpf, only reticulospinal cell clusters and hindbrain motoneurons still express *trpc3* (Fig. 4L). Expression drastically changes on the fifth day of development when it becomes confined to cerebellar regions including the cerebellar plate (CeP) and the valvula cerebelli (Va; Fig. 4M, N).

RT-PCR and immunohistochemical analysis in mice located TRPC3 in the whole brain with especially high levels in cerebellar Purkinje cells (Huang et al., 2007; Hartmann et al., 2008). Interestingly, mGluR1-mediated slow mixed-cation excitatory postsynaptic conductance is abolished in TRPC3 deficient mice, leading to a phenotype showing impairment of motor control and coordination (Rodríguez-Santiago et al., 2007; Hartmann et al., 2008; Becker et al., 2009). The fact that transcripts of all type I mGluRs (most prominently *mglur1a*) have been located to the zebrafish cerebellar region (Haug et al., 2012) suggests that mGluR1 signaling upstream of TRPC3 is a conserved mechanism.

Transcript distribution of *trpc4* paralogs

Despite 70% sequence homology between the two zebrafish *trpc4* paralogs their expression patterns are very distinct and hardly overlapping, suggesting non-redundant functions. We found *trpc4a* to be expressed in the olfactory bulb (Fig. 5A-C). This is in line with observations showing that TRPC4 expression is especially high in the murine OB (Zechel et al., 2007; Dong et al., 2012). Detection of two types of group I mGluR transcripts (*mglur1a* and *-5b*) in zebrafish OB granule cells (Haug et al., 2012) raises the appealing possibility that TRPC4 channels could function downstream of these GPCRs and hence be implicated in modulation of odor signal processing. This hypothesis is further supported by findings showing that mGluR5 participates in the regulation of excitability of murine OB granule cells (Heinbockel et al., 2007), and that group I mGluRs are involved in synchronization and generation of slow rhythmic oscillations in the OB glomerular network (Dong et al., 2009). In

addition, there is recent evidence that TRPC4 can be activated in an ionotropic NMDA-receptor-dependent pathway in OB granule cells (Stroh et al., 2012).

Cells expressing *trpc4b* mRNA are first observed in the trigeminal nuclei as early as 24 hpf (Fig. 5 D, E). By 48 hpf, staining appears in the pallial region (Fig. 5 H, J). In early larvae, *trpc4b* expression in the head has expanded to additional cranial sensory ganglia, including now the trigeminal, glossopharyngeal and vagal ganglia (Fig. 5 K, L). While expression spreads to neurons in all epibranchial ganglia at the fifth day of development, pallial expression is downregulated (Fig. 5 N). Up to 3 dpf, high transcript levels are also apparent in Rohon-Beard neurons (RB, Fig. 5 F, G, M).

RB neurons are a transient cell population, which is only present until approximately 3 dpf before they are replaced by dorsal root ganglia (DRGs) (Bernhardt et al., 1990). Interestingly, quantitative RT-PCR analyses showed expression in trigeminal ganglia and additionally significant variations in the mRNA levels of TRPC4 between DRGs isolated from different segments of adult mice suggesting functional variability (Vandewauw et al., 2013). Both cell types, trigeminal and RB neurons, convey diverse sensory information delivered to the trunk and tail regions (Clarke et al., 1984; Sneddon, 2003). If and how TRPC4 is involved in somatosensory information processing in zebrafish is an interesting topic for future investigations.

Expression of *trpc5*

Cloning of the *trpc5a* paralog was reported previously by Petko and colleagues (Petko et al., 2009). Their study aimed at identifying binding partners of neuronal calcium sensor-1, which is involved in inner ear development. However, no *trpc5a* expression was detected in the zebrafish ear. In analogy to their data, we found *trpc5a* transcripts in a subset of motoneurons in the hindbrain (Fig. 6A-C). By 48 hpf, diffuse staining is visible in large parts of the diencephalon and in the caudal region of the telencephalon (Fig. 6C, D). In the hindbrain, a distinct pattern in various nuclei becomes apparent, probably including populations of reticulospinal neurons (Fig. 6D, F). In early larvae, expression in the eye can

be detected most pronounced in the GCL, but also at lower levels in the INL (Fig. 6E). By 5 dpf, expression has spread to large parts of the brain, most prominently in the mid- and hindbrain. Widespread expression in the hindbrain, including a population of motoneurons located in rhombomere 8, can now be observed, however, the strongest staining is still seen in the nuclei of putative reticulospinal neurons. While riboprobes are now absent in the telencephalon, pronounced expression has started bilaterally in both habenulae (Fig. 6G, H).

Expression of the *trpc5b* paralog is weak and diffuse during the first two days of development. Transcripts can be detected in large parts of the diencephalon, but also in the telencephalon and the hindbrain but to a weaker extend (Fig. 6J, K). This expression remains essentially unchanged on the third day but additional staining can be detected in the retinal INL (Fig. 6L). By 5dpf, retinal expression has become more prominent (Fig. 6M), and staining in two distinct bilateral midbrain and hindbrain nuclei is visible (see asterisks in Fig. 6N, O).

Based on studies in different model systems, a role in regulation of neurite length and growth cone morphology has been proposed for TRPC5 (summarized in Vennekens et al., 2012). The widespread distribution of both zebrafish orthologs in the embryonic and larval brain is consistent with such a function in neuronal development. We also found both *trpc5* paralogs to be expressed in a similar pattern as *trpc1* in the zebrafish retina. There seems to be at least a partial overlap of these different channel subunits in the inner retina. Interestingly, the distribution of *trpc5* paralogs differs with *trpc5a* showing elevated expression in the GCL and *trpc5b* being restricted to the INL, while *trpc1* is equally expressed in both of these retinal layers. In general, there appears to be a functionally important overlap of *trpc5a* and *trpc1* expression domains also in other tissues (compare Fig. 6J-O with Fig.2). This raises the possibility of heteromere formation by these two channel subunits. In heterologous expression systems, such an interaction has been demonstrated to form a functional channel with unique electrophysiological properties, distinct from any other *trpc* homomere (Strübing et al., 2001).

Expression pattern of *trpc6* paralogs

Several mutations in human TRPC6 have been linked to kidney pathologies such as familial focal segmental glomerulosclerosis (Winn et al., 2005). In zebrafish, an earlier study failed to detect substantial levels of *trpc6a* transcripts in the kidney but could locate *trpc6a* expression to the head, pectoral fins, aortic endothelial cells and gastrointestinal smooth muscle cells (Möller et al., 2008). We could not detect any *trpc6* expression during the first two days of development. We found expression in the gut and the cloaca in early larvae (Fig. 7A, B), however no staining in the pectoral fins and the aorta was observed. By 5 dpf, *trpc6a* mRNA staining was visible in the heart ventricle (Fig. 7C). Recent reports indicate that TRPC channels may play a key role in regulation of cardiac pacemaking, ventricular activity, and contractility in the developing chick heart (Sabourin et al., 2011). Furthermore, TRPC channels have been linked to several heart diseases including cardiac hypertrophy and heart failure (reviewed in Watanabe et al., 2009).

Expression of *trpc6b* is restricted to two clusters in the hindbrain, likely the anterior and posterior motor nuclei of branchiomeric nerve V (Fig. 7D-G). This expression pattern is already visible at 24 hpf and remains stable up to 3 dpf. On the fifth day of development, expression of *trpc6b* is not detectable anymore. The temporally restricted expression of *trpc6b* points to a possible role in development. Axons arising from the two bilateral trigeminal motor nuclei located in the hindbrain innervate the mandibular arch muscles (Higashijima et al., 2000). In neural cell culture experiments using rat pheochromocytoma 12 cells, TRPC6 and TRPC1 have been reported to balance neurite outgrowth velocity thereby maintaining optimal conditions for establishing functional neuronal networks (Kumar et al., 2012). Axonal outgrowth from the zebrafish trigeminal motor neurons starts at approximately 28 hpf and they reach their targets at around 72 hpf (Higashijima et al., 2000), matching the timing of *trpc6b* expression.

Transcript distribution of the *trpc7* paralogs

TRPC7 is the most recently cloned member of the canonical subfamily of TRP channels. In mice, northern blot analysis demonstrated high expression levels in the heart, lung, and eye. Tissue samples from the brain, spleen, and testes contain lower levels of TRPC7 mRNA (Okada et al., 1999). Expression of human TRPC7 is highly enriched in the pituitary and kidney, but was also found in brain tissues by RT-PCR (Riccio et al., 2002).

Zebrafish TRPC7 has not been characterized previously. We identified two paralogs with non-overlapping expression patterns. A small subset of cells located in the proximal part of the ventral OE expresses *trpc7a* (Fig. 8A-H). These cells presumably represent a subpopulation of OSNs distinct from the *trpc2a*- or *trpc2b*-expressing population (compare Fig. 8A-H with Fig 3). The expression starts on the first day of development and is maintained at least up to 5 dpf. Between 2 and 3 dpf, *trpc7a* transcripts are transiently observed in some midbrain cell clusters (see asterisks in Fig. 8C, D, F).

While expression of *trpc7b* is first found bilaterally in the dorsal telencephalic region 24 hpf (Fig. 8J, K), expression domains including bilateral nuclei in the diencephalon as well as reticulospinal cell clusters and motoneurons in the hindbrain were observed in later developmental stages (Fig. 8L-O). Starting at 3 dpf, a prominent staining in the rostral hindbrain is detected (Fig. 8N, O). Most expression domains vanish after 3 dpf but the hindbrain cell clusters persist at least until 5 dpf (Fig. 8P).

Comparing our expression analysis to previously published reports (Okada et al., 1999; Riccio et al., 2002) suggests that *trpc7* expression in the brain is conserved among vertebrates. It has been reported that TRPC7 prefers to form heteromers and builds for example functional channels with TRPC1 and TRPC3 in heterologous expression systems (Lievremont et al., 2004; Zagranichnaya et al., 2005). A recent study suggested that a heteromeric TRPC6/7 channel is involved in the depolarization of intrinsically photosensitive retinal ganglion cells (Xue et al., 2011). These specialized cells serve in the retina for non-image forming visual functions, such as the entrainment of biological rhythms. However, the existence of equivalent cells in the zebrafish retina is still under debate (Matos-Cruz et al., 2011). As several *trpc* channels show overlapping expression domains with *trpc7* in

zebrafish, heteromeric channel formation seems likely. Unfortunately, functional studies of TRPC7 might be complicated by this fact.

Various aspects of sensory and motor processing in developing zebrafish seem to rely partially on signaling through canonical TRP channels. The dynamic spatial and temporal expression patterns of *trpc*s hint at an involvement in developmental processes. Table 1 represents an overview of zebrafish *trpc* expression in all examined stages. Interestingly, with the exception of *trpc6a*, the detectable expression of the entire zebrafish *trpc* subfamily seems to be confined to the nervous system during development even though the possibility of an expression in non-neural structures cannot be completely ruled out. Notably, maybe with the exception of broadly expressed *trpc5* genes, all other identified *trpc* paralogs show an entirely non-overlapping expression pattern strongly arguing for neo- and/or subfunctionalization events during zebrafish evolution (Postlethwait, 2007). However, functional studies of TRPC channels have not been done so far, and it remains to be determined where functional shifts indeed occur in this animal.

EXPERIMENTAL PROCEDURES

Fish maintenance and breeding

Zebrafish (*Danio rerio*) were kept at a 14:10 hours light/dark cycle at 28°C as previously described (Westerfield, 2007). Embryos of WIK wild-type fish were raised in E3 medium containing 0.01% methylene blue as well as 0.2 mM PTU (1-phenyl-2-thiourea; Sigma-Aldrich) to avoid pigmentation.

Annotation of *trpc* cDNAs

As gene predictions within GenBank are produced by automated processes which have been shown to contain numerous errors, *trpc* cDNA sequences used in this study were manually annotated. Sequences were identified and annotated using combined information from expressed sequence tags and genome databases (GenBank, http://www.ncbi.nlm.nih.gov; Ensembl, http://www.ensembl.org/index.html). Human and mouse sequences were used as initial query (for more details on sequence annotation see Gesemann et al., 2010).

Phylogeny

The phylogenetic analysis was performed on the Phylogeny.fr platform (http://www.phylogeny.fr/) comprising the following steps (Dereeper et al., 2008). Sequences were aligned using MUSCLE (v3.7) (Edgar, 2004) configured for highest accuracy (MUSCLE with default settings). Sequences length varied between 793 and 1602 amino acids. After alignment, ambiguous regions (i.e. containing gaps and/or poorly aligned) were removed using Gblocks (v0.91b) (Castresana, 2000). The following parameters were implemented. The minimum length of a block after gap cleaning was set to 5; positions with a gap in less than 50% of the sequences were selected in the final alignment if they were within an appropriate block; all segments with contiguous nonconserved positions bigger than 8 were rejected; minimum number of sequences for a flank position were 55%. After curation 451 amino acids were chosen for further analysis. The phylogenetic tree was reconstructed using

the maximum likelihood method implemented in the PhyML program (v3.0 aLRT) (Guindon and Gascuel, 2003). The default substitution model was selected assuming an estimated proportion of invariant sites (of 0.000) and 4 gamma-distributed rate categories to account for rate heterogeneity across sites. The gamma shape parameter was estimated directly from the data (gamma=0.728). Reliability for internal branch was assessed using the aLRT test (Anisimova and Gascuel, 2006). Graphical representation and edition of the phylogenetic tree were performed with TreeDyn (v198.3) and the svg file imported into CoralDraw (version X5; Coral Corporation Ottawa, Canada) for final editing.

Cloning of *trpc* genes and *in situ* probe synthesis:

Total RNA was extracted from WIK larvae at 5 dpf using the RNeasy Mini kit (Qiagen) and cDNA was synthesized using the SuperScript II Reverse Transcriptase kit (Invitrogen) following the manual. To isolate sequences of interest from each *trpc* gene, specific primers were designed and used for polymerase chain reaction (PCR) amplification with the Jump Start Taq Polymerase kit (Sigma). Forward and reverse primers for PCR amplification of *in situ* probes are listed in table 2. Appropriately sized PCR products were purified with the Nucleo Spin Extract II kit (Macherey-Nagel) and subcloned into the pCR II vector (TOPO TA Cloning Kit, Invitrogen). The resultant plasmids were transformed into TOP10 *Escherichia coli* cells, and at least three independent clones were sequenced to confirm annotated *trpc* sequences. Our sequences were subsequently submitted to GenBank under the following accession numbers: *trpc1* KF446627, *trpc2a* KF446628, *trpc2b* KF446629, *trpc3* KF446630, *trpc4a* KF446631, *trpc4b* KF446632, *trpc5a* KF446633, *trpc5b* KF446634, *trpc6a* KF446635, *trpc6b* KF446636, *trpc7a* KF446637, and *trpc7b* KF446638. Plasmids were linearized with the appropriate restriction enzymes and sense and antisense *in vitro* transcription for RNA probe preparation was performed in the presence of digoxigenin (DIG) coupled nucleotides (Roche). Longer RNA probes (*trpc2a* and *b*; *trpc3*; *trpc4a* and *b*) were subsequently hydrolyzed with 200mM Na_2Co_3 and 200 mM $NaHCO_3$ to yield fragments of about 500-600

nucleotides in length. For *in situ* hybridization experiments, probes were diluted to a concentration of approximately 4ng/μl.

Whole mount *in situ* hybridization

Whole mount *in situ* hybridization was performed as described by (Thisse and Thisse, 2008) with the following adaptations. Larvae 3 and 5 dpf were permeabilized by proteinase K treatment for one hour and 90 minutes, respectively. Temperature for hybridization and stringency washes was 65°C for all probes. 1% Roche blocking reagent was used for blocking and dilution of alkaline-phosphatase-conjugated anti-DIG antibody (Roche) 1:5000. The staining solution contained 1mM levamisol in order to quench endogenous peroxidase activity.

Imaging:

To enhance visibility under the microscope, the yolk was gently removed prior to mounting on an adapted glass slide in 100% glycerol. Images of embryos were taken using a light microscope (BX61, Olympus) with DIC filter and a CCD camera (ColorView III, Olympus). Adobe Photoshop and Adobe Illustrator software were used to adjust levels and assemble figures, respectively.

ACKNOWLEDGMENTS

We would like to thank Kara Dannenhauer for expert maintenance of zebrafish and technical assistance, and members of our laboratory for discussion.

REFERENCES

Abramowitz J, Birnbaumer L. 2009. Physiology and pathophysiology of canonical transient receptor potential channels. FASEB J. 23:297–328.

Albert AP. 2011. Gating mechanisms of canonical transient receptor potential channel proteins: role of phosphoinositols and diacylglycerol. Adv Exp Med Biol 704:391–411.

Anisimova M, Gascuel O. 2006. Approximate likelihood-ratio test for branches: A fast, accurate, and powerful alternative. Syst Biol 55:539–552.

Becker EBE, Oliver PL, Glitsch MD, Banks GT, Achilli F, Hardy A, Nolan PM, Fisher EMC, Davies KE. 2009. A point mutation in TRPC3 causes abnormal Purkinje cell development and cerebellar ataxia in moonwalker mice. Proc Natl Acad Sci U S A 106:6706–6711.

Bernhardt RR, Chitnis AB, Lindamer L, Kuwada JY. 1990. Identification of spinal neurons in the embryonic and larval zebrafish. J. Comp. Neurol. 302:603–616.

Bezzerides VJ, Ramsey IS, Kotecha S, Greka A, Clapham DE. 2004. Rapid vesicular translocation and insertion of TRP channels. Nat Cell Biol 6:709–720.

Castresana J. 2000. Selection of conserved blocks from multiple alignments for their use in phylogenetic analysis. Mol Biol Evol 17:540–552.

Cheng W, Sun C, Zheng J. 2010. Heteromerization of TRP channel subunits: extending functional diversity. Protein Cell 1:802–810.

Clapham DE. 2003. TRP channels as cellular sensors. Nature 426:517–524.

Clarke JD, Hayes BP, Hunt SP, Roberts A. 1984. Sensory physiology, anatomy and immunohistochemistry of Rohon-Beard neurones in embryos of Xenopus laevis. J. Physiol. (Lond.) 348:511–525.

Damann N, Voets T, Nilius B. 2008. TRPs in our senses. Curr. Biol. 18:R880-9.

Dereeper A, Guignon V, Blanc G, Audic S, Buffet S, Chevenet F, Dufayard J, Guindon S, Lefort V, Lescot M et al. 2008. Phylogeny.fr: robust phylogenetic analysis for the non-specialist. Nucleic Acids Res 36:W465-9.

Dong H, Davis JC, Ding S, Nai Q, Zhou F, Ennis M. 2012. Expression of transient receptor potential (TRP) channel mRNAs in the mouse olfactory bulb. Neurosci. Lett. 524:49–54.

Dong H, Hayar A, Callaway J, Yang X, Nai Q, Ennis M. 2009. Group I mGluR activation enhances Ca(2+)-dependent nonselective cation currents and rhythmic bursting in main olfactory bulb external tufted cells. J. Neurosci. 29:11943–11953.

Dulac C, Torello AT. 2003. Molecular detection of pheromone signals in mammals: from genes to behaviour. Nat. Rev. Neurosci. 4:551–562.

Edgar RC. 2004. MUSCLE: multiple sequence alignment with high accuracy and high throughput. Nucleic Acids Res 32:1792–1797.

Gesemann M, Lesslauer A, Maurer CM, Schonthaler HB, Neuhauss SCF. 2010. Phylogenetic analysis of the vertebrate excitatory/neutral amino acid transporter (SLC1/EAAT) family reveals lineage specific subfamilies. BMC Evol Biol 10:117.

Gilliam JC, Wensel TG. 2011. TRP channel gene expression in the mouse retina. Vision Res. 51:2440–2452.

Gleason E. 2012. The influences of metabotropic receptor activation on cellular signaling and synaptic function in amacrine cells. Vis. Neurosci. 29:31–39.

Guindon S, Gascuel O. 2003. A simple, fast, and accurate algorithm to estimate large phylogenies by maximum likelihood. Syst Biol 52:696–704.

Hartmann J, Dragicevic E, Adelsberger H, Henning HA, Sumser M, Abramowitz J, Blum R, Dietrich A, Freichel M, Flockerzi V et al. 2008. TRPC3 channels are required for synaptic transmission and motor coordination. Neuron 59:392–398.

Hashiguchi Y, Furuta Y, Nishida M. 2008. Evolutionary patterns and selective pressures of odorant/pheromone receptor gene families in teleost fishes. PLoS ONE 3:e4083.

Haug MF, Gesemann M, Mueller T, Neuhauss SCF. 2012. Phylogeny and expression divergence of metabotropic glutamate receptor genes in the brain of zebrafish (Danio rerio). J. Comp. Neurol.

Heinbockel T, Laaris N, Ennis M. 2007. Metabotropic glutamate receptors in the main olfactory bulb drive granule cell-mediated inhibition. J. Neurophysiol. 97:858–870.

Higashijima S, Hotta Y, Okamoto H. 2000. Visualization of cranial motor neurons in live transgenic zebrafish expressing green fluorescent protein under the control of the islet-1 promoter/enhancer. J. Neurosci. 20:206–218.

Huang W, Young JS, Glitsch MD. 2007. Changes in TRPC channel expression during postnatal development of cerebellar neurons. Cell Calcium 42:1–10.

Koike C, Obara T, Uriu Y, Numata T, Sanuki R, Miyata K, Koyasu T, Ueno S, Funabiki K, Tani A et al. 2010. TRPM1 is a component of the retinal ON bipolar cell transduction channel in the mGluR6 cascade. Proc. Natl. Acad. Sci. U.S.A. 107:332–337.

Kumar S, Chakraborty S, Barbosa C, Brustovetsky T, Brustovetsky N, Obukhov AG. 2012. Mechanisms controlling neurite outgrowth in a pheochromocytoma cell line: the role of TRPC channels. J. Cell. Physiol. 227:1408–1419.

Kunert-Keil C, Bisping F, Krüger J, Brinkmeier H. 2006. Tissue-specific expression of TRP channel genes in the mouse and its variation in three different mouse strains. BMC Genomics 7:159.

Lev S, Katz B, Minke B. 2012. The activity of the TRP-like channel depends on its expression system. Channels (Austin) 6:86–93.

Leypold BG, Yu CR, Leinders-Zufall T, Kim MM, Zufall F, Axel R. 2002. Altered sexual and social behaviors in trp2 mutant mice. Proc. Natl. Acad. Sci. U.S.A. 99:6376–6381.

Lievremont J, Bird GSJ, Putney JW, JR. 2004. Canonical transient receptor potential TRPC7 can function as both a receptor- and store-operated channel in HEK-293 cells. Am J Physiol Cell Physiol 287:C1709-16.

Liman ER, Corey DP, Dulac C. 1999. TRP2: a candidate transduction channel for mammalian pheromone sensory signaling. Proc. Natl. Acad. Sci. U.S.A. 96:5791–5796.

Liman ER, Innan H. 2003. Relaxed selective pressure on an essential component of pheromone transduction in primate evolution. Proc. Natl. Acad. Sci. U.S.A. 100:3328–3332.

Lucas P, Ukhanov K, Leinders-Zufall T, Zufall F. 2003. A diacylglycerol-gated cation channel in vomeronasal neuron dendrites is impaired in TRPC2 mutant mice: mechanism of pheromone transduction. Neuron 40:551–561.

Matos-Cruz V, Blasic J, Nickle B, Robinson PR, Hattar S, Halpern ME, Nitabach MN. 2011. Unexpected Diversity and Photoperiod Dependence of the Zebrafish Melanopsin System. PLoS ONE 6:e25111.

Meyer A, van de Peer Y. 2005. From 2R to 3R: evidence for a fish-specific genome duplication (FSGD). Bioessays 27:937–945.

Minke B. 2010. The history of the Drosophila TRP channel: the birth of a new channel superfamily. J. Neurogenet. 24:216–233.

Möller CC, Mangos S, Drummond IA, Reiser J. 2008. Expression of trpC1 and trpC6 orthologs in zebrafish. Gene Expr. Patterns 8:291–296.

Morgans CW, Zhang J, Jeffrey BG, Nelson SM, Burke NS, Duvoisin RM, Brown RL. 2009. TRPM1 is required for the depolarizing light response in retinal ON-bipolar cells. Proc. Natl. Acad. Sci. U.S.A. 106:19174–19178.

Nilius B, Owsianik G. 2011. The transient receptor potential family of ion channels. Genome Biol 12:218.

Okada T, Inoue R, Yamazaki K, Maeda A, Kurosaki T, Yamakuni T, Tanaka I, Shimizu S, Ikenaka K, Imoto K et al. 1999. Molecular and functional characterization of a novel mouse transient receptor potential protein homologue TRP7. Ca(2+)-permeable cation channel that is constitutively activated and enhanced by stimulation of G protein-coupled receptor. J Biol Chem 274:27359–27370.

Petko JA, Kabbani N, Frey C, Woll M, Hickey K, Craig M, Canfield VA, Levenson R. 2009. Proteomic and functional analysis of NCS-1 binding proteins reveals novel signaling pathways required for inner ear development in zebrafish. BMC Neurosci 10:27.

Postlethwait JH. 2007. The zebrafish genome in context: ohnologs gone missing. J. Exp. Zool. B Mol. Dev. Evol. 308:563–577.

Putney JW. 2004. The enigmatic TRPCs: multifunctional cation channels. Trends Cell Biol. 14:282–286.

Ramsey IS, Delling M, Clapham DE. 2006. An introduction to TRP channels. Annu. Rev. Physiol. 68:619–647.

Riccio A, Medhurst AD, Mattei C, Kelsell RE, Calver AR, Randall AD, Benham CD, Pangalos MN. 2002. mRNA distribution analysis of human TRPC family in CNS and peripheral tissues. Brain Res Mol Brain Res 109:95–104.

Rodríguez-Santiago M, Mendoza-Torres M, Jiménez-Bremont JF, López-Revilla R. 2007. Knockout of the trcp3 gene causes a recessive neuromotor disease in mice. Biochem. Biophys. Res. Commun. 360:874–879.

Roussigne M, Blader P, Wilson SW. 2012. Breaking symmetry: the zebrafish as a model for understanding left-right asymmetry in the developing brain. Dev Neurobiol 72:269–281.

Sabourin J, Robin E, Raddatz E. 2011. A key role of TRPC channels in the regulation of electromechanical activity of the developing heart. Cardiovasc. Res. 92:226–236.

Sato Y, Miyasaka N, Yoshihara Y. 2005. Mutually exclusive glomerular innervation by two distinct types of olfactory sensory neurons revealed in transgenic zebrafish. J. Neurosci. 25:4889–4897.

Selvaraj S, Sun Y, Singh BB. 2010. TRPC channels and their implication in neurological diseases. CNS Neurol Disord Drug Targets 9:94–104.

Shapovalov G, Lehen'kyi V, Skryma R, Prevarskaya N. 2011. TRP channels in cell survival and cell death in normal and transformed cells. Cell Calcium 50:295–302.

Shen Y, Heimel JA, Kamermans M, Peachey NS, Gregg RG, Nawy S. 2009. A transient receptor potential-like channel mediates synaptic transmission in rod bipolar cells. J. Neurosci. 29:6088–6093.

Sneddon LU. 2003. Trigeminal somatosensory innervation of the head of a teleost fish with particular reference to nociception. Brain Res 972:44–52.

Soboloff J, Spassova M, Hewavitharana T, He LP, Luncsford P, Xu W, Venkatachalam K, van Rossum D, Patterson RL, Gill DL. 2007. TRPC channels: integrators of multiple cellular signals. Handb Exp Pharmacol:575–591.

Sorensen PW, Stacey NE. 2004. Brief review of fish pheromones and discussion of their possible uses in the control of non□indigenous teleost fishes. New Zealand Journal of Marine and Freshwater Research 38:399–417.

Stowers L, Holy TE, Meister M, Dulac C, Koentges G. 2002. Loss of sex discrimination and male-male aggression in mice deficient for TRP2. Science 295:1493–1500.

Stroh O, Freichel M, Kretz O, Birnbaumer L, Hartmann J, Egger V. 2012. NMDA receptor-dependent synaptic activation of TRPC channels in olfactory bulb granule cells. J. Neurosci. 32:5737–5746.

Strübing C, Krapivinsky G, Krapivinsky L, Clapham DE. 2001. TRPC1 and TRPC5 form a novel cation channel in mammalian brain. Neuron 29:645–655.

Tai Y, Feng S, Du W, Wang Y. 2009. Functional roles of TRPC channels in the developing brain. Pflugers Arch. 458:283–289.

Thisse C, Thisse B. 2008. High-resolution in situ hybridization to whole-mount zebrafish embryos. Nat Protoc 3:59–69.

Touhara K, Vosshall LB. 2009. Sensing odorants and pheromones with chemosensory receptors. Annu. Rev. Physiol. 71:307–332.

Vandewauw I, Owsianik G, Voets T. 2013. Systematic and quantitative mRNA expression analysis of TRP channel genes at the single trigeminal and dorsal root ganglion level in mouse. BMC Neurosci 14:21.

Venkatachalam K, Montell C. 2007. TRP channels. Annu. Rev. Biochem. 76:387–417.

Vennekens R, Menigoz A, Nilius B. 2012. TRPs in the Brain. Rev. Physiol. Biochem. Pharmacol. 163:27–64.

Watanabe H, Murakami M, Ohba T, Ono K, Ito H. 2009. The pathological role of transient receptor potential channels in heart disease. Circ. J. 73:419–427.

Westerfield M. 2007. The zebrafish book: A guide for the laboratory use of zebrafish (Danio rerio). 5th ed. Eugene: University of Oregon Press.

Winn MP, Conlon PJ, Lynn KL, Farrington MK, Creazzo T, Hawkins AF, Daskalakis N, Kwan SY, Ebersviller S, Burchette JL et al. 2005. A mutation in the TRPC6 cation channel causes familial focal segmental glomerulosclerosis. Science 308:1801–1804.

Xue T, Do MTH, Riccio A, Jiang Z, Hsieh J, Wang HC, Merbs SL, Welsbie DS, Yoshioka T, Weissgerber P et al. 2011. Melanopsin signalling in mammalian iris and retina. Nature 479:67–73.

Yu P, Gu S, Bu J, Du J. 2010. TRPC1 is essential for in vivo angiogenesis in zebrafish. Circ. Res. 106:1221–1232.

Zagranichnaya TK, Wu X, Villereal ML. 2005. Endogenous TRPC1, TRPC3, and TRPC7 proteins combine to form native store-operated channels in HEK-293 cells. J Biol Chem 280:29559–29569.

Zechel S, Werner S, Bohlen Und Halbach O von. 2007. Distribution of TRPC4 in developing and adult murine brain. Cell Tissue Res. 328:651–656.

FIGURES

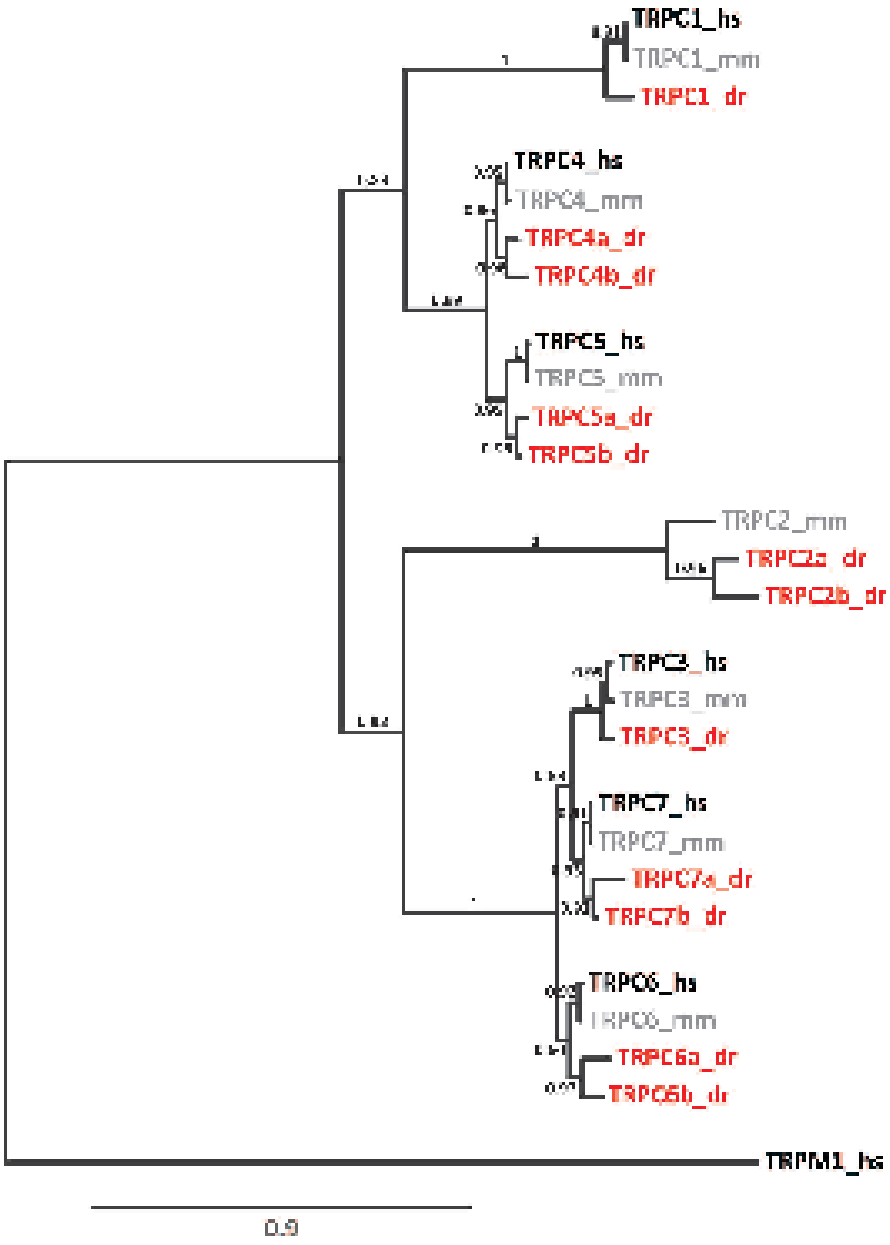

Figure 1: Several of the zebrafish *trpc* genes have retained duplicates. TRPC amino acid sequences of the following species were used in phylogenetic reconstructions (hs = *Homo sapiens*; mm = *Mus musculus* and dr = *Danio rerio*). While zebrafish TRPCs are shown in red, mouse TRPCs are given in light gray and human TRPCs in dark gray. The human TRPM1 gene, which shares about 20% homology with human TRPC5, was used as an outgroup to root the tree. Note that except *trpc1* and *trpc3* the zebrafish has retained gene duplicates for all other *trpc*s.

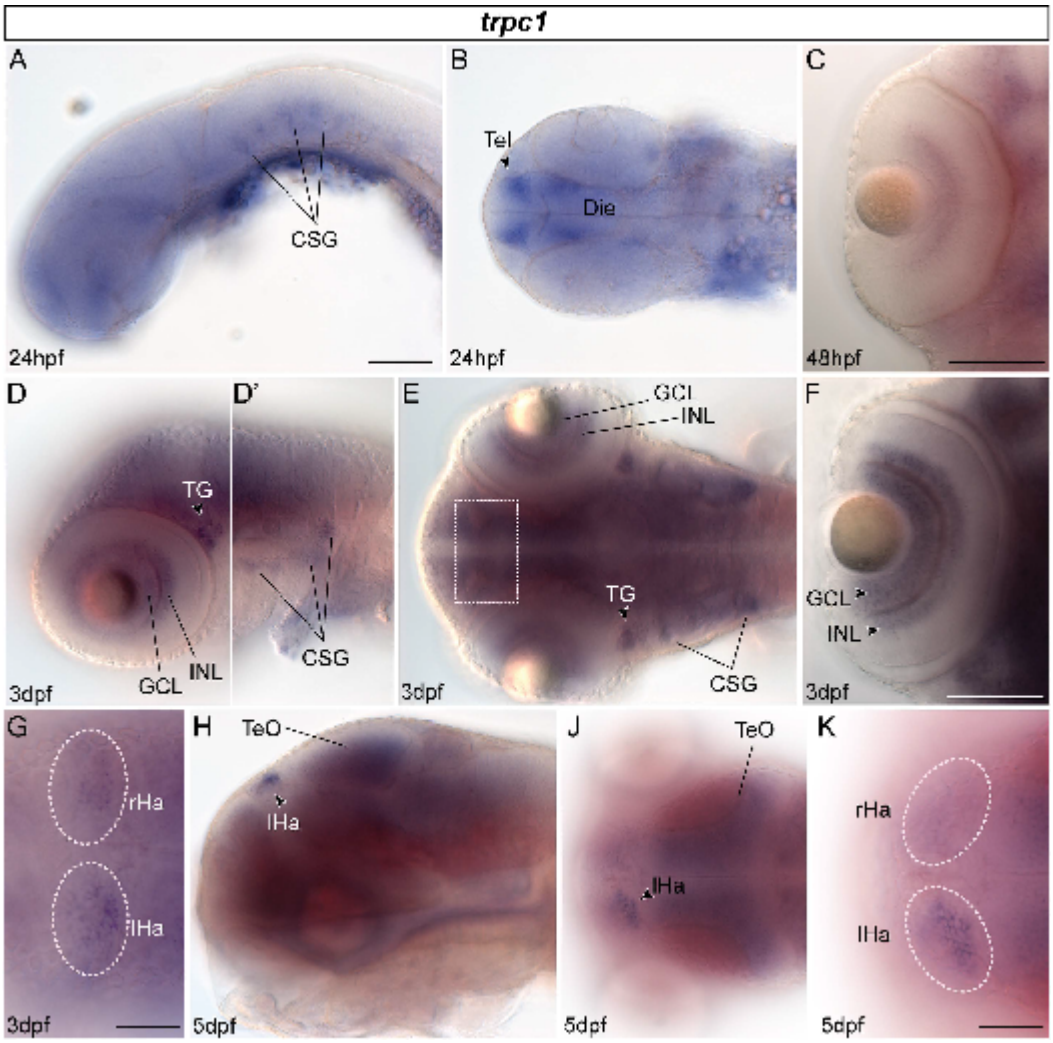

Figure 2: Expression patterns of *trpc1* in whole mount zebrafish. **A** Dorsal view of embryonic brain expression 24 hpf. **B** Lateral close-up of *trpc1* expression in CSG 24 hpf. **C** Expression of *trpc1* in the 48 hpf retinal neuroepithelium in higher magnification; anterior points to the top. **D** Lateral view of a larva 3 dpf is shown with different focal planes in D and D'. **E** Dorsal view; boxed region is shown in G. **F** Staining in the eye of larvae 3dpf; anterior is up. **G** Focus on expression in the habenulae 3dpf in a dorsal view corresponding to the boxed region in E. Note the differential expression in the left (lHa) and right (rHa) habenula. **H** Brain staining in a larva 5 dpf is shown in a lateral view. **J, K** Dorsal views on larvae 5 dpf. More cells expressing *trpc1* are present in the left compared to the right habenula. Anterior is to the left unless otherwise stated. CSG = cranial sensory ganglia; Die = diencephalon; GCL = ganglion cell layer; INL = inner nuclear layer; Tel = telencephalon; TeO = optic tectum; TG = trigeminal ganglia. Scale bars of 100µm are indicated in the first picture of a series until changed. The scale bars in G and K refer to 50 µm.

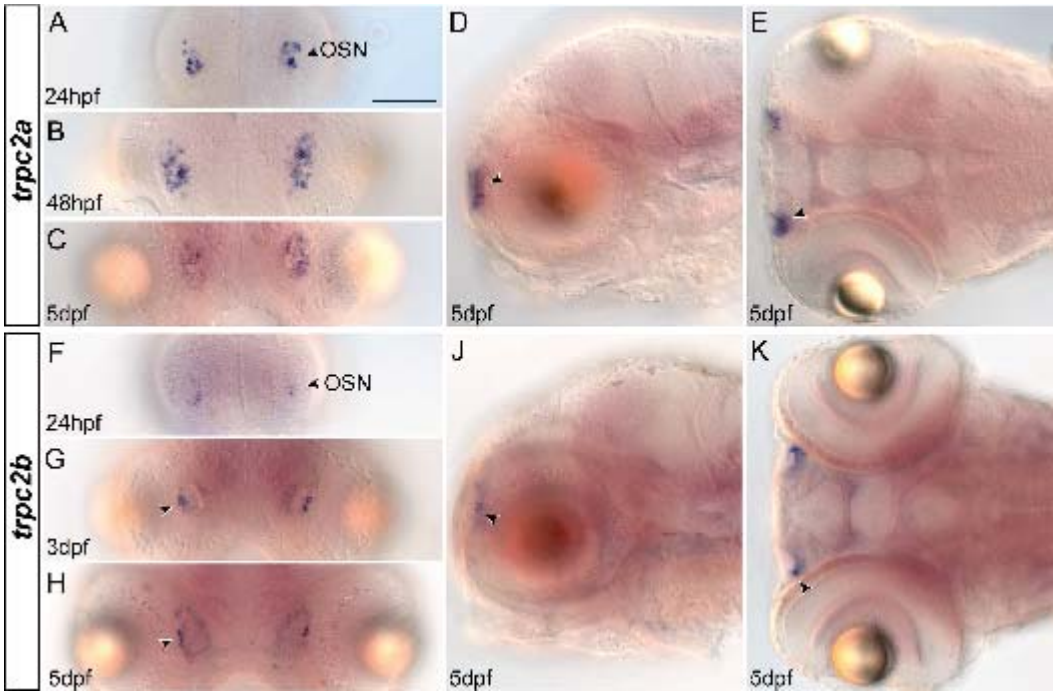

Figure 3: Expression of zebrafish *trpc2* paralogs in the olfactory system. **A-E** Images show transcript localization of *trpc2a* in the olfactory epithelium in frontal (A-C), lateral (D) and dorsal (E) views at the developmental stages indicated. **F-K** Expression of *trpc2b* in a distal subpopulation of olfactory sensory neurons (OSNs) shown in frontal (F-H), lateral (J) and dorsal (K) whole mount views. Scale bar in A = 100µm applies to all pictures shown.

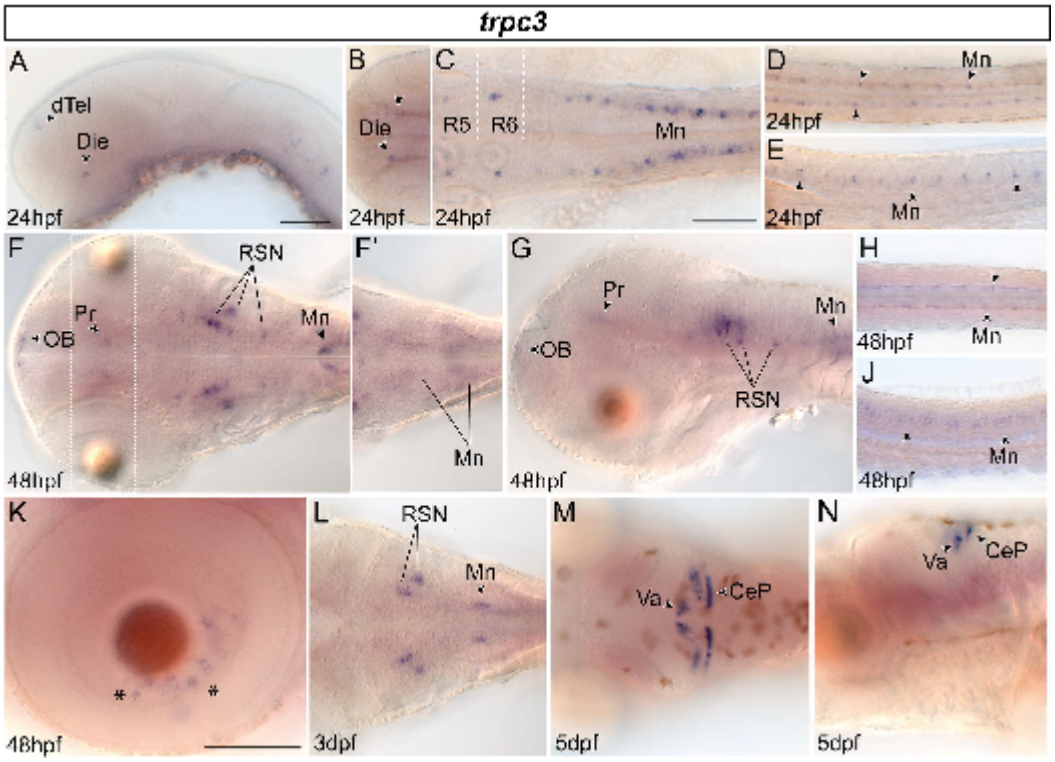

Figure 4: Dynamic *trpc3* expression in zebrafish whole mounts. **A** shows an embryo 24hpf expressing *trpc3* in different forebrain clusters. **B** The bilateral neural clusters in the diencephalon expressing *trpc3* are shown from dorsal. **C** Dorsal view of the hindbrain region. Dashed lines mark approximate boundaries of rhombomeres 5 and 6 (R5, R6). **D, E** Dorsal (D) and lateral (E) views of zebrafish tail region 24 hpf with expression in motoneurons. **F, G** Expression in the brain at 48 hpf. Dotted field in F shows the same embryo in a different focal plane. F' depicts a more dorsal plane of the hindbrain region. **H, J** *trpc3* staining in motoneurons 48 hpf in dorsal (H) and lateral (J) views. **K** Lateral view on retinal cells (asterisks) expressing *trpc3* transiently around 48 hpf. **L** Hindbrain expression of *trpc3* in larvae 3 dpf. **M, N** Cerebellar cell clusters expressing *trpc3* at 5 dpf shown in dorsal (M) and lateral (N) views. Anterior is always left. CeP = cerebellar plate; Die = diencephalon; dTel = dorsal telencephalon; Mn = motoneurons; OB = olfactory bulb; Pr = pretectum; RSN = reticulospinal neurons; Va = valvula cerebelli. Scale bar in A (for all pictures without scale bar), C and K = 100µm.

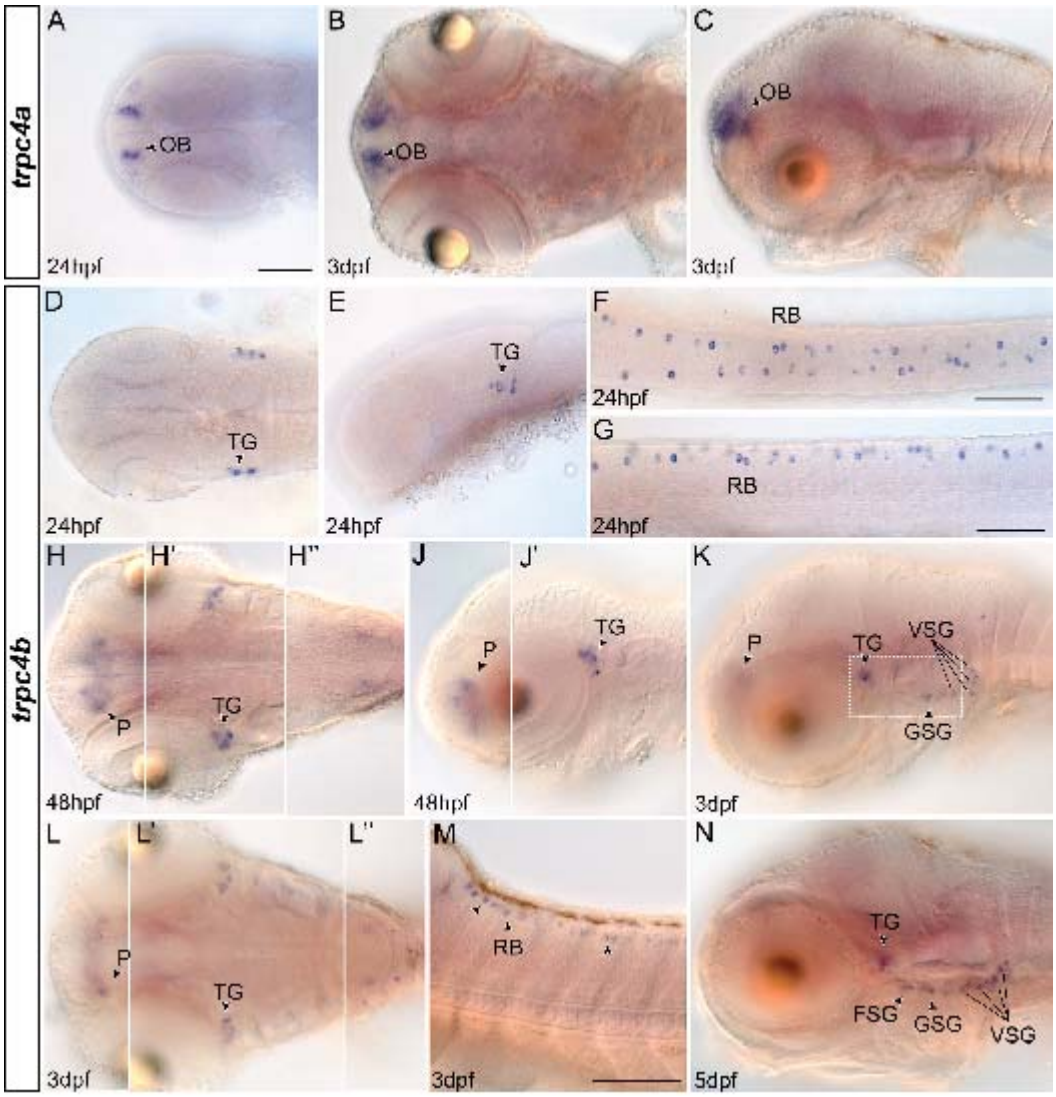

Figure 5: Expression patterns of *trpc4* paralogs during development. **A-C** Expression of *trpc4a* was exclusively found in the olfactory bulb. Dorsal (A, B) and lateral (C) views of representative embryonic and larval stages are shown. **D-G** Images showing *trpc4b* staining in embryonic head (D, E) and tail (F, G) region 24 hpf were taken dorsally (D, F) and laterally (E, G). **H, J** Whole mount zebrafish 48 hpf, shown in dorsal (H) and lateral (J) views. Prime figures show the same embryo in different focal planes. **K-M** Lateral (K, M) and dorsal (L) views on *trpc4b* expression in 3 dpf whole mount larvae. Dotted box in K has a more lateral focal plane compared to core image. L' and L'' show different focal planes compared to the larva in L. **N** Expression of *trpc4b* spreads to all cranial sensory ganglia (CSG) around 5 dpf. Anterior is always left. FSG = facial sensory ganglia; GSG = glossopharyngeal sensory ganglia ; OB = olfactory bulb; P = pallium; RB = Rohon-Beard neurons; TG = trigeminal ganglia; VSG = vagal sensory ganglia. Scale bar in A (applies to all images if not otherwise indicated), F, G and M = 100µm.

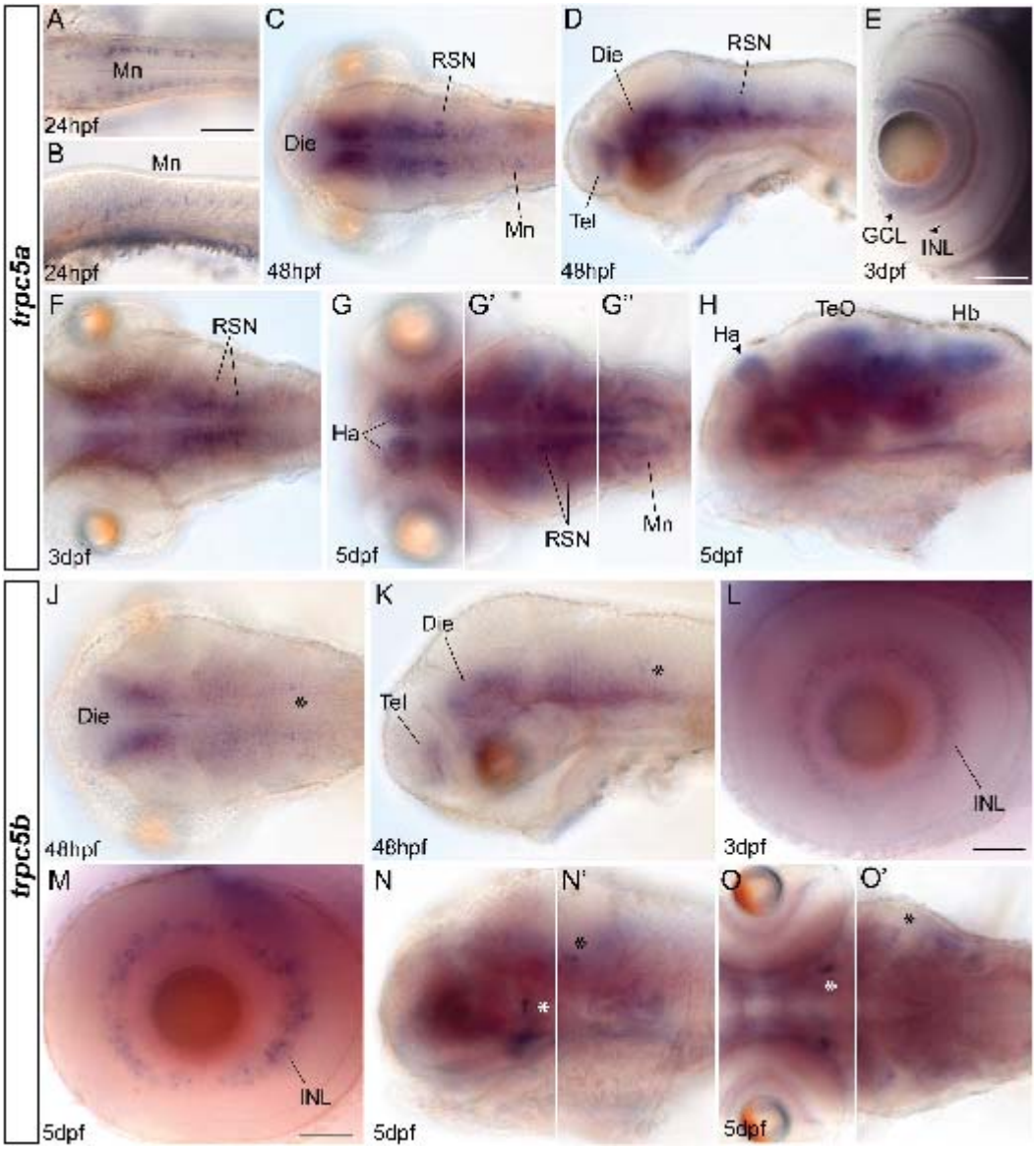

Figure 6: Transcript distribution of *trpc5a* (A-H) and *trpc5b* (J-O). **A, B** Dorsal (A) and lateral (B) views on the hindbrain region of 24 hpf embryos. **C, D** *trpc5a* expression in brain regions and spinal cord of zebrafish 48 hpf shown dorsally (C) and laterally (D). **E** Retinal expression in 3 dpf larvae, anterior is up. **F** Dorsal view on hindbrain region showing expression in reticulospinal neurons (RSNs) at 3 dpf. **G, H** Dorsal (G) and lateral (H) views on 5 dpf larvae with G, G' and G'' showing different focal planes. **J, K** Expression of *trpc5b* in the diencephalon and hindbrain (see asterisks). J and K show dorsal and lateral views, respectively. **L** and **M** are lateral views on retinal *trpc5b* expression. **N, O** Lateral and dorsal views of whole mount *in situ* staining with asterisks labeling brain regions expressing *trpc5b* 5 dpf. Prime images show different focal planes of the same larvae as in N and O, respectively. Die = diencephalon; GCL = ganglion cell layer; Ha = habenula; Hb = hindbrain; INL = inner nuclear layer; Mn = motoneurons; Tel = telencephalon; TeO = optic tectum. Scale bar in A (for all images without scale bar) = 100µm. Scale bar in E, L and M = 50µm.

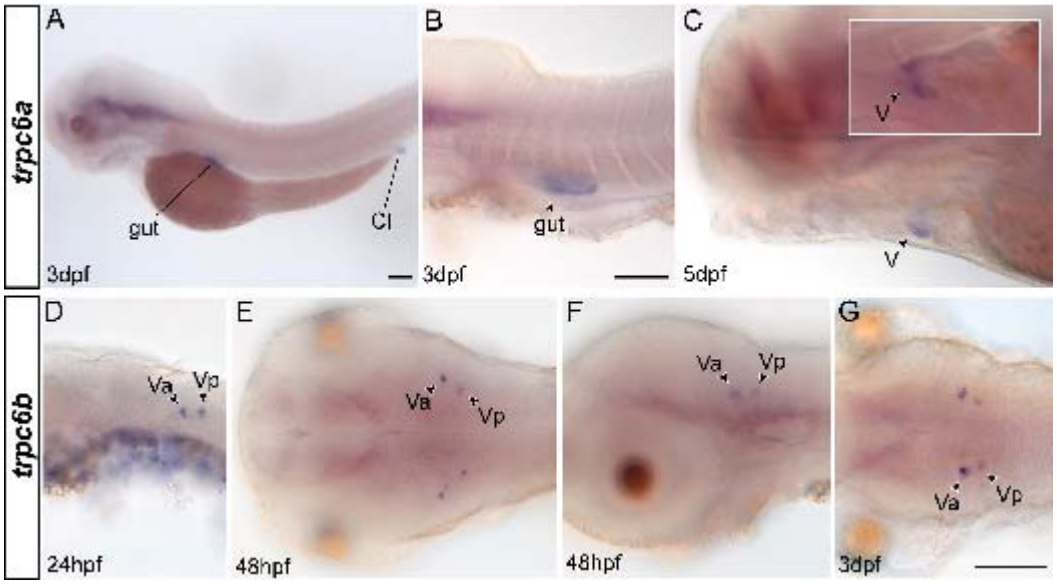

Figure 7: Expression pattern of *trpc6a* (A-C) and *trpc6b* (D-G). *trpc6a* expression is not detectable before 3 dpf. **A** Overview of WISH in a larva 3dpf. **B** Expression of *trpc6a* in the gut is shown in a lateral view. **C** The heart ventricle (V) expresses the gene, too. Insert is a ventral view on the heart to compare with the lateral view in the main image. **D** Expression of *trpc6b* is present in the hindbrain region 24 hpf, lateral view. **E, F** Expression of *trpc6b* in embryos 48 hpf shown in a dorsal (E) and a lateral (F) view. **G** Dorsal head view on the expression in larvae 3 dpf. Anterior is always left. Cl = cloaca; Va = anterior clusters of trigeminal motor neurons; Vp = posterior clusters of trigeminal motor neurons. Scale bar in A (for all pictures of not otherwise indicated), B and G = 100µm.

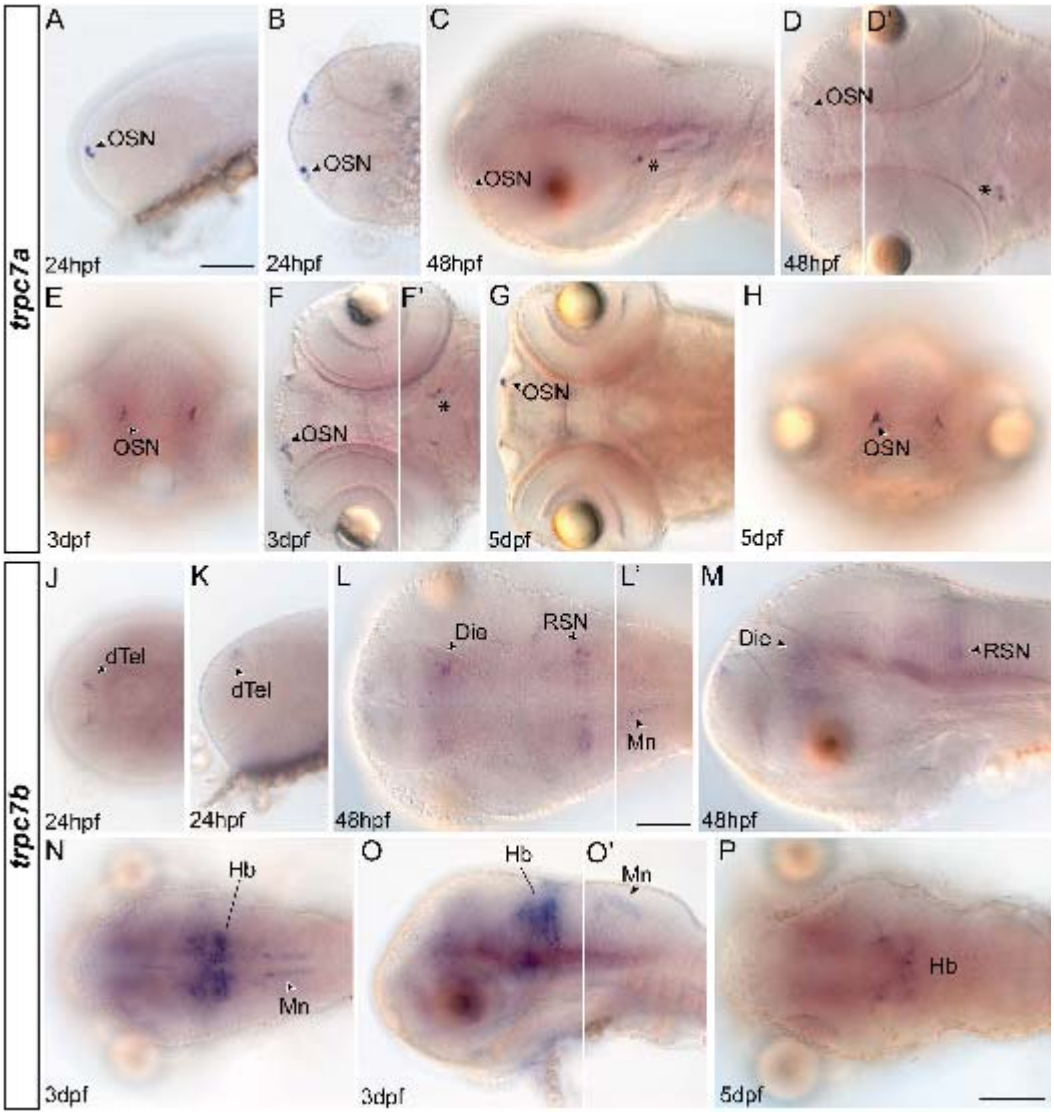

Figure 8: Whole mount in situ hybridization of zebrafish *trpc7a* (A-H) and *trpc7b* (J-P). **A-D** *trpc7a* expressing olfactory sensory neurons (OSNs) in embryos shown laterally (A,C) and dorsally (B,D). Asterisks mark expression domains in the midbrain. The focal plane in D' differs from D. **E, F** Frontal (E) and ventral (F) views on 3 dpf whole mount larvae, F' shows a different focus to F. Asterisk in F' labels midbrain cell clusters expressing *trpc7a* transiently. **G, H** Dorsal (G) and frontal (H) views on larvae 5 dpf. **J, K** Dorsal (J) and lateral (K) view of the telencephalic cell clusters expressing *trpc7b* in embryos 24 hpf. **L, M** Expression of *trpc7b* as detected in zebrafish 48 hpf shown in dorsal (L) and lateral (M) views. Focus in L' is more dorsal compared to L. **N, O** Expression in 3 dpf larvae, shown in dorsal (N) and lateral (O, O') views. **P** Dorsal whole mount view on *trpc7b* expression in larvae 5 dpf. Die = diencephalon; dTel = dorsal telencephalon; Hb = hindbrain; Mn = motoneurons; RSN = reticulospinal neurons. Scale bar in A (applies to all images without scale bar), L', P = 100µm.

TABLES

Table 1: Overview of zebrafish *trpc* expression domains during the first five days of development. Mammalian expression from references cited in the text was added for comparisons.

Gene	24hpf	48hpf	3dpf	5dpf	Mammalian mRNA expression
trpc1	brain (ubiquitous), cranial sensory ganglia (CSG)	brain (ubiquitous), cranial sensory ganglia, retinal neuroepithelium	brain (ubiquitous), cranial sensory ganglia, retina: ganglion cell layer (GCL) and inner nuclear layer (INL)	brain (ubiquitous), cranial sensory ganglia, retina: ganglion cell layer and inner nuclear layer	brain, kidney, lung, skeletal muscle (Kunert-Keil et al., 2006), retina (Gilliam and Wensel, 2011), ubiquitous (Nilius and Owsianik, 2011)
trpc2a	olfactory sensory neurons (microvillous)	olfactory sensory neurons (microvillous)	olfactory sensory neurons (microvillous)	olfactory sensory neurons (microvillous)	mouse vomeronasal sensory neurons (Liman et al., 1999)
trpc2b	olfactory sensory neurons	olfactory sensory neurons	olfactory sensory neurons	olfactory sensory neurons	
trpc3	dorsal telencephalon (dTel), diencephalon, rhombomeres 5/6, motoneurons (Mn)	pretectum (Pr), olfactory bulb (OB), retinal neuroepithelial cells, reticulospinal neurons (RSN), motoneurons	reticulospinal neurons, motoneurons	cerebellum (CeP & Va)	brain (Huang et al., 2007; Hartmann et al., 2008)
trpc4a	olfactory bulb	olfactory bulb	olfactory bulb	olfactory bulb	brain (Vennekens et al., 2012), olfactory bulb (Zechel et al., 2007; Dong et al., 2012), trigeminal and dorsal root ganglia (Vandewauw et al., 2013)
trpc4b	trigeminal ganglia (TG), Rohon-Beard neurons (RB)	pallium (P), trigeminal ganglia, Rohon-Beard neurons	pallium, cranial sensory ganglia, Rohon-Beard neurons	cranial sensory ganglia	

trpc5a	motoneurons	brain, reticulospinal neurons, motoneurons	brain, reticulospinal neurons, motoneurons, retina: INL, GCL	brain, reticulospinal neurons, motoneurons, retina: INL, GCL	Whole brain, especially fetal brain (summarized in Nilius and Owsianik, 2011; Vennekens et al., 2012)
trpc5b	brain	brain	brain, retina: INL	brain, retina: INL	
trpc6a	no expression detectable	no expression detectable	gut, cloaca (Cl)	heart ventricle (V)	brain, heart, kidney, lung, smooth muscle cells (Kunert-Keil et al., 2006), spleen, ovary, small intestine, neutrophils (reviewed in Nilius and Owsianik, 2011)
trpc6b	trigeminal motor nuclei	trigeminal motor nuclei	trigeminal motor nuclei	no expression detectable	
trpc7a	olfactory sensory neurons	olfactory sensory neurons, midbrain cell cluster	olfactory sensory neurons, midbrain cell cluster	olfactory sensory neurons	Pituitary, kidney, heart, lung, brain (Okada et al., 1999; Riccio et al., 2002)
trpc7b	dispersed neural clusters in the brain	brain, reticulospinal neurons, motoneurons	brain, reticulospinal neurons, motoneurons	hindbrain nuclei	

Table 2: Primer list for the generation of *in situ* hybridization probes. *trpc1*, *trpc5a*, *trpc5b,* and *trpc6a* have two probes, which were both used in WISH experiment.

Gene	Forward primer 5'-3'	Reverse primer 5'-3'	Length
trpc1 probe 1	TCAGTGCTTTGCCGTATTC	CTTGGCAAGTTCTTCATAATC	776 bp
trpc1 probe2	CTGCTAGTGCTCATCTCTTTC	CATGCTGGGTCACTTTAAA	836 bp
trpc2a	GCACGTTCCAAGCTTTAC	CGGATTTAATTGTAATATTGTG	1490 bp
trpc2b	CGAACCACTTGGAAACTG	GCTTGTTTTTCAGGAATGG	1618 bp
trpc3	GGTCTTCGGGAGCAAAC	CAGTGCTGATGCTCATGG	1535 bp
trpc4a	GTGGGATGGTGGATTTCAG	CCGTGGTTACAAAAGAAAG	2518 bp
trpc4b	GAACTCAGACTGCAAAAACG	CTGCTAGTTTCACCTTCATTTC	2611 bp
trpc5a probe1	CTCAAGGAGCTCAGCAAAG	GGCGATGGCAAACAAAG	778 bp
trpc5a probe2	GCCAAGGGCGTCTCTTTC	AGGATCGGTTGTCGTTAAG	799 bp
trpc5b probe1	TGTGCCGTCTCATTCAAAG	CTACGCGCCTGATCAAGAAG	816 bp
trpc5b probe2	AGAGCCCAACAACTGCAAAG	CAAGCCTGTGGTTTCTTTC	1755 bp
trpc6a probe1	GAAAGGATGAATCAAAGAAGAG	CAAGGATGCGAGCTCATTG	874 bp
trpc6a probe2	CGGCCTCCTTTACTATTTTC	CGATGACCACTGTGACATTG	1816 bp
trpc6b	CGCTGACCGTTTTGAAG	GCGATGAGCATGTTGAGTAAG	1786 bp
trpc7a	ATGGTCTTTCTTGCCTTCATG	GCTCTAGGACACTTTCAGCTAC	1836 bp
trpc7b	ACCACCCTGCGAGAGAAG	AGAACGCCCACCACAAAG	791 bp